

Mixed-order transition in the antiferromagnetic quantum Ising chain in a field

Péter Lajkó^{1,*} and Ferenc Igloi^{2,3,†}

¹Department of Physics, Kuwait University, P.O. Box 5969, Safat 13060, Kuwait

²Wigner Research Centre for Physics, Institute for Solid State Physics and Optics, H-1525 Budapest, P.O. Box 49, Hungary

³Institute of Theoretical Physics, Szeged University, H-6720 Szeged, Hungary



(Received 15 December 2020; revised 6 March 2021; accepted 20 April 2021; published 4 May 2021)

The antiferromagnetic quantum Ising chain has a quantum critical point which belongs to the universality class of the transverse Ising model (TIM). When a longitudinal field (h) is switched on, the phase transition is preserved, which turns to first order for $h/\Gamma \rightarrow \infty$, Γ being the strength of the transverse field. Here we will re-examine the critical properties along the phase transition line. During a quantum block renormalization group calculation, the TIM fixed point for $h/\Gamma > 0$ is found to be unstable. Using DMRG techniques, we calculated the entanglement entropy and the spin-spin correlation function, both of which signaled a divergent correlation length at the transition point with the TIM exponents. At the same time, the bulk correlation function has a jump and the end-to-end correlation function has a discontinuous derivative at the transition point. Consequently for finite h/Γ the transition is of mixed order.

DOI: [10.1103/PhysRevB.103.174404](https://doi.org/10.1103/PhysRevB.103.174404)

I. INTRODUCTION

Quantum phase transitions are among the fundamental problems of modern physics, the properties of which are studied in different disciplines: solid state physics, quantum field theory, quantum information, and statistical mechanics [1]. Quantum phase transitions take place at $T = 0$ temperature and these are indicated by singularities in the ground-state expectation values of some observables by varying a control parameter, such as the strength of a transverse field. There are several model systems which have been experimentally realized by ultracold atoms in an optical lattice [2]. One of such basic problems is the antiferromagnetic Ising chain in a mixed transverse and longitudinal field. The Hamiltonian of the model is defined as

$$\hat{H} = \sum_{i=1}^L J \sigma_i^z \sigma_{i+1}^z - \sum_{i=1}^L \Gamma \sigma_i^x - h \sum_{i=1}^L \sigma_i^z, \quad (1)$$

in terms of the $\sigma_i^{x,z}$ Pauli matrices at site i . In the experimental setup the longitudinal fields are not too strong [3].

Theoretically, the quantum phase transition in this model has been studied by different methods: finite-size exact diagonalization by the Lanczos method [4], density matrix renormalisation (DMRG) [5,6], quantum Monte Carlo simulations [7], and the fidelity susceptibility method [8]. The limiting case $h/J \rightarrow 2$ and $\Gamma \rightarrow 0$ is studied in Ref. [9] and a generalization with an m -spin product term, i.e., replacing $\sigma_i^z \sigma_{i+1}^z$ by $\prod_{j=0}^{m-1} \sigma_{i+j}^z$ is studied in Refs. [10–12]. Recently, the model with quenched disorder, in which $J_i > 0$ and Γ_i are i.i.d. random numbers, but the $h_i = h$ are nonrandom, has also been studied [6,7].

The phase diagram of the clean system in Eq. (1) is calculated through the extrapolated position of the maximum of the entanglement entropy, as described in Sec. III A 1. It is shown in Fig. 1 in terms of J/Γ vs h/Γ . This has two exactly solved points, which are denoted by TIM and CEP, respectively. In the absence of longitudinal field, $h = 0$, there is an antiferromagnetic (AFM) ordered phase, for $J/\Gamma > 1$, which is separated from the paramagnetic (PM) phase by a continuous phase transition point, at $J_c/\Gamma = 1$ which belongs to the universality class of the transverse Ising model (TIM) [13]. In the vicinity of the transition point the excitation energy (inverse correlation length) $\epsilon \sim 1/\xi$ vanishes as

$$\epsilon \sim J - J_c, \quad J \geq J_c, \quad (2)$$

thus the gap (correlation length) exponent is $\nu = 1$. The AFM order is characterized by the spin-spin correlation function:

$$C(r) = (-1)^r \langle \sigma_i^z \sigma_{i+r}^z \rangle, \quad (3)$$

which is translational invariant for periodic chains. At the phase-transition point $C(r)$ has a power-law decay:

$$C(r) \sim r^{-\eta}, \quad (4)$$

with $\eta = 1/4$. The second exactly solved point is at $J/\Gamma \rightarrow \infty$ and $h/\Gamma \rightarrow \infty$, in which quantum fluctuations are negligible. Here the phase transition takes place at the classical endpoint (CEP), at $h/J = 2$ between an AFM phase and a ferromagnetic (FM) phase and the transition is of first order. At the CEP the ground state is infinitely degenerate; the entropy per site is finite [14].

Our interest in this work is the behavior of the system between the two exactly solved points, for $0 < h/\Gamma < \infty$. Here the phase diagram contains an AFM ordered phase for strong enough couplings, $J/\Gamma > J_c/\Gamma$. At the other side of the phase-transition line, for $J/\Gamma < J_c/\Gamma$ there is a ferromagnetic

*peter.lajko@ku.edu.kw

†igloi.ferenc@wigner.hu

(FM) order in the system, which is maintained by the longitudinal field. This is evident at $J = 0$, in which case $C(r) = (-1)^r[(\Gamma/h)^2 + 1]^{-1}$. In previous studies [5,9] the excitation spectrum of the system has been investigated and a vanishing gap is found at the phase-transition line, $J = J_c$, signaling a divergent correlation length. According to precise numerical results the gap vanishes in the same way as for the TIM in Eq. (2). Due to this result it is generally believed that the phase transition for $0 < h/\Gamma < \infty$ belongs to the TIM universality class.

With this claim, however, there are still some unclear points. It was not investigated how the correlation function behaves when passing the phase transition line from the AFM-ordered phase. At $h/\Gamma = 0$ it stays zero in the complete PM phase, but for $h/\Gamma > 0$ it should become ferromagnetic at some point. It is of interest how this transition from AFM to FM orders occurs. A further question is how this transition is connected with the first-order one at the CEP in the transition line. It is also interesting, whether this transition is symmetric or not, at least in terms of the critical exponents at the two sides of the transition. Another open question concerns the scaling behavior of the entanglement entropy in the vicinity of the phase transition point.

Our aim in this article is to examine and clarify the above issues. First, we studied the stability of the TIM fixed point in relation to switching on the longitudinal field. For this we used an approximate quantum block renormalization group (RG) method and let vary the size of the block. More precise numerical results are obtained from a DMRG calculation. We investigated the scaling properties of the entanglement entropy in the phase-transition region and studied the divergence of the related correlation length. In extensive numerical work the spin-spin correlation function is calculated and its properties are analyzed, both for bulk spins and for end-to-end correlations.

The rest of the paper is organized in the following way. In Sec. II we introduce and apply the quantum block RG method to test the stability of the fixed point of the TIM. The DMRG results are presented in Sec. III, first about the scaling behavior of the entanglement entropy in Sec. III A and afterwards about the correlation function in Sec. III B. Our paper is closed with a discussion in Sec. IV.

II. QUANTUM RG TREATMENT

Renormalization of quantum systems started with the celebrated paper by Wilson about the Kondo problem [15]. For lattice models a real space version, the so-called block transformation method has been introduced [16] and applied for a set of (mainly one-dimensional) problems [17]. In this method the system is divided into blocks and the parameters of the Hamiltonian are separated to intra- and interblock terms. Solving the block Hamiltonian exactly by numerical methods the lowest states are retained and identified as states of the block-spin variable, while the renormalized values of the interblock parameters are obtained by (first-order) perturbation calculation. Due to the used approximations the block RG method generally provides rather poor results with the smallest block size ($n = 2$), however, using larger blocks the results can be improved. This has been shown for the TIM [18,19] among

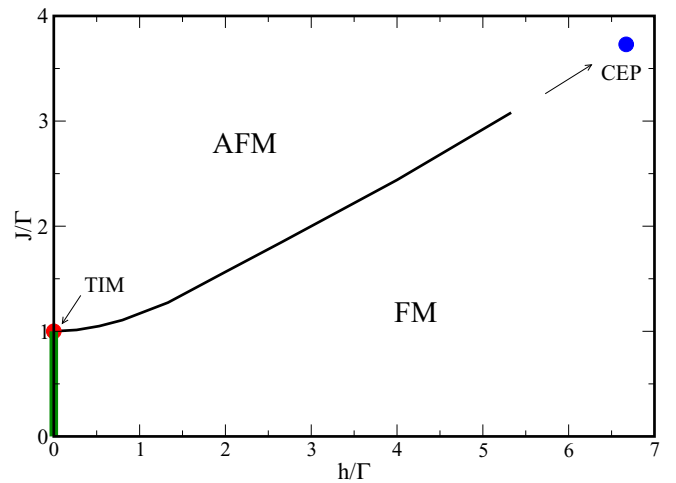


FIG. 1. The zero-temperature phase diagram of the Ising chain with antiferromagnetic coupling J , in transverse (Γ) and longitudinal (h) magnetic fields calculated by the DMRG method. In the absence of longitudinal field, $h = 0$, the transition between a quantum antiferromagnetic (AFM) phase and a quantum paramagnetic (PM) phase (indicated by thick green line) is controlled by the fixed point of the transverse Ising model (TIM) at $(J/\Gamma = 1, h/\Gamma = 0)$. For finite value of $h > 0$ the AFM phase survives and at the other side of the phase boundary there is a quantum ferromagnetic (FM) phase. In the classical limit, $\Gamma = 0$, thus $J/\Gamma \rightarrow \infty$ and $h/\Gamma \rightarrow \infty$ there is a classical endpoint (CEP) at $(h/J = 2)$ having a first-order transition.

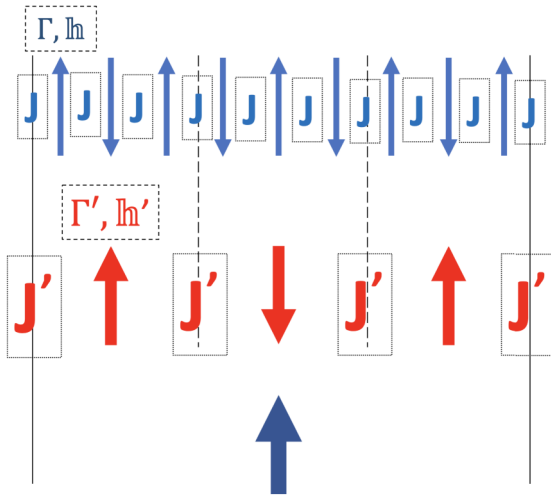
others, i.e., with the Hamiltonian in Eq. (1) in the absence of a longitudinal field, $h = 0$.

Here in our treatment we include the longitudinal field, both in the Hamiltonian and in the RG transformations. In particular we are interested in the stability of the TIM fixed point by switching on the longitudinal field. Since at the CEP there are no quantum fluctuations our quantum RG can't describe the behavior of the system around that classical point. In this procedure the length of the blocks n is an *odd number* in order to preserve the antiferromagnetic order in the system. During renormalization the block of spins is replaced by a single renormalized Ising spin variable, which is illustrated in Fig. 2. For this the block Hamiltonian is solved exactly and from its spectrum the two lowest eigenstates are retained. The renormalized values of the parameters are obtained from the condition that the matrix elements are equal in the original and in the renormalized basis.

In the actual calculation first we perform a gauge transformation, $\sigma_i^z \rightarrow (-1)^j \sigma_i^z$, and make a rotation $x \leftrightarrow z$, thus the intrablock Hamiltonian of n spins is written as

$$\hat{H}_B = - \sum_{i=1}^{n-1} J \sigma_i^x \sigma_{i+1}^x - \sum_{i=1}^n \Gamma \sigma_i^z - h \sum_{i=1}^n (-1)^j \sigma_i^x. \quad (5)$$

We solve the ground state ($|0\rangle$) and the first excited state ($|1\rangle$) of \hat{H}_B with energies ϵ_0 and ϵ_1 , respectively. We also calculate the matrix elements: $m_x(i) = \langle 0 | \sigma_i^x | 1 \rangle$ and $m_z(i) = \langle 0 | \sigma_i^z | 0 \rangle$,


 FIG. 2. Illustration of the block renormalization for $n = 3$.

which are called x and z magnetizations, respectively. For the block the total magnetizations are $M_x = \sum_{i=1}^n m_x(i)$ and $M_z = \sum_{i=1}^n m_z(i)$.

The renormalized value of the coupling follows from

$$J' = Jm_x(1)m_x(n). \quad (6)$$

The renormalized values of the transverse (Γ') and the longitudinal fields (h') are related with the value of the gap:

$$\sqrt{(\Gamma')^2 + (h')^2} = \frac{\epsilon_1 - \epsilon_0}{2}. \quad (7)$$

In addition we require that the ratio of the total x and z magnetizations M_x/M_z remains the same after the transformation. This leads to the relation:

$$\frac{\Gamma'}{h'} = \frac{M_x}{M_z}. \quad (8)$$

We have iterated the RG equations in Eqs. (6), (7), and (8), which has two trivial fixed points. The one at $(J/\Gamma = 0, h/\Gamma = 0)$ controls the disordered phase, while the other at $(J/\Gamma = \infty, h/\Gamma = 0)$ is for the ordered phase. The transition between these phases are controlled by two nontrivial fixed points. The first, denoted by $FP1$ is located at $(J/\Gamma)_1 > 0$ and $(h/\Gamma)_1 = 0$ is the TIM fixed point. Without longitudinal field ($h = 0$) its properties have been studied earlier in details [18,19]. Here we are interested in its stability with respect to switching on the longitudinal field. The second nontrivial fixed point $FP2$ is located at $(J/\Gamma)_2 > 0$ and $(h/\Gamma)_2 > 0$. At the nontrivial fixed points we have calculated the eigenvalues of the linearized transformation, $\lambda_1 > \lambda_2$ from which the scaling exponents follows as $y_{1,2} = \frac{\ln \lambda_{1,2}}{\ln n}$. As usual, for $y > 0$ ($y < 0$) the fixed point is repulsive (attractive). For $FP2$ we found $\lambda_2 < 0$, which means rotation of the trajectory in the vicinity of the fixed point. This behavior is related to the quantum nature of the RG, which cannot describe a first-order transition between classical states at CEP. We have also calculated the dynamical exponent z from the scaling of the energy at the fixed point: $\Gamma' = n^{-z}\Gamma$. For different values of the size of the block, $n = 3, 5, 7, 9, 11$, and 13 the calculated critical parameters are collected in Tables I and II. Regarding $FP1$ the critical parameters (except y_2) agree with the previous

 TABLE I. Critical parameters at the $FP1$ fixed point calculated with different sizes of the block n .

n	$(J/\Gamma)_1$	$(h/\Gamma)_1$	y_1	y_2	z
3	0.8660	0.	0.763	0.011	0.631
5	0.9262	0.	0.833	0.119	0.704
7	0.9496	0.	0.863	0.169	0.741
9	0.9619	0.	0.879	0.198	0.763
11	0.9694	0.	0.890	0.217	0.779
13	0.9745	0.	0.898	0.230	0.791
∞	1.	0.	1.	—	1.

calculations in Refs. [18,19]. The exact results, which are obtained for $n \rightarrow \infty$ and presented in the last row of Table I are approached logarithmically, having a correction $\sim 1/\ln n$. The new feature of this calculation is the second exponent y_2 , due to the presence of the longitudinal field. Since $y_2 > 0$, according to our RG approach $h > 0$ is a relevant perturbation, thus the critical properties of the complete model should be different from the TIM. Having a look at the block-size dependence of y_2 it smoothly increases with n ; for small sizes this grows approximately as $\sim 0.09 \ln n$.

As seen in Table II for the position of $FP2$, that $(J/\Gamma)_2 \approx (J/\Gamma)_1$, while $(h/\Gamma)_2$ decreases with n . For small block sizes we have an approximate relation $(h/\Gamma)_2 \sim 1.15/\ln n$. The leading critical index y_1 slowly decreases with n and it is approximately the same at both fixed points. We can conclude the results of this approximate investigation, that the critical behavior of the model for $h > 0$ is probably not controlled by the TIM fixed point, but some critical indices are still very close to the quantum Ising values. We expect more accurate information from DMRG studies.

III. DMRG RESULTS

The complete phase diagram of the model has been studied numerically by the DMRG method. In this investigation we used finite samples of length up to $L = 1024$; their ground state and the first few excited states are calculated. Here the original version of the finite system DMRG scheme was utilized with periodic and open boundary conditions [20,21]. For the correlations it was systematically and carefully checked that their values are vastly independent of the basis size m within the error bars. The accuracy of the ground-state energy calculations was in the range of 10^{-6} – 10^{-8} and this was in

 TABLE II. Critical parameters at the $FP2$ fixed point calculated with different sizes of the block n .

n	$(J/\Gamma)_2$	$(h/\Gamma)_2$	y_1	λ_2	z
3	1.1052	0.8998	1.052	0.114	0.640
5	1.0079	0.6830	0.955	−0.042	0.657
7	0.9791	0.5852	0.939	−0.140	0.667
9	0.9672	0.5243	0.916	−0.216	0.673
11	0.9617	0.4808	0.899	−0.279	0.677
13	0.9591	0.4473	0.887	−0.333	0.681

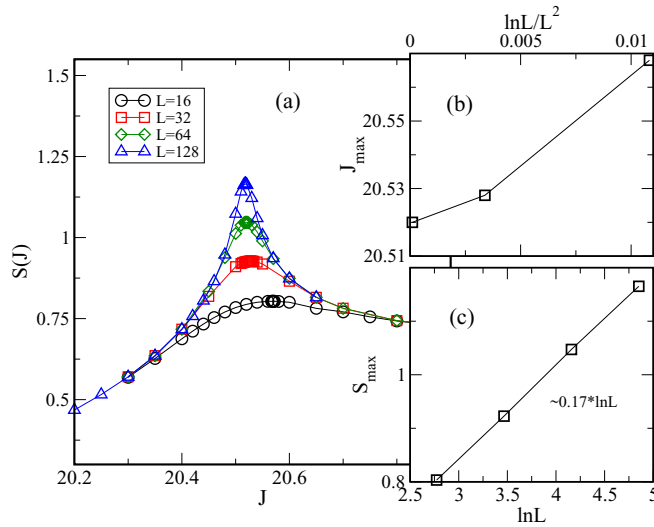


FIG. 3. (a) The J dependence of the entanglement entropy at $h = 40.0$ and $\Gamma = 1.5$ for different lengths of periodic chains. The position of the maximum is shifted by $\sim \ln L/L^2$ from the phase transition point; see in (b). The value at the maximum scales as $\approx 0.17 \ln L$; see in (c).

full agreement with the truncation error, the largest basis size being $m = 140$ – 260 for the different systems.

In general we have fixed the value of the transverse field to $\Gamma = 1.5$ and used different values of the longitudinal field: $h = 0.0, 0.4, 0.8, 2.0, 10.0, 20.0$, and 40.0 . By varying the strength of the coupling we have studied the behavior of the correlation function, $C(L/2 - 1) = -\langle \sigma_1^z \sigma_{L/2-1}^z \rangle$, as well as the entanglement entropy \mathcal{S} calculated between the two halves of the chain. Particular attention is paid to the properties of the system in the vicinity of the phase transition point.

A. Entanglement entropy

If we divide the chain into two parts of lengths ℓ and $L - \ell$, then the entanglement between the two parts is quantified by the von Neumann entropy:

$$S_\ell = -\text{Tr}(\rho_\ell \ln \rho_\ell) = -\text{Tr}(\rho_{L-\ell} \ln \rho_{L-\ell}) = S_{L-\ell}. \quad (9)$$

Here $\rho_\ell = \text{Tr}_{L-\ell} \rho$ and $\rho_{L-\ell} = \text{Tr}_\ell \rho$ is the reduced density matrix with $\rho = |\phi\rangle\langle\phi|$ and $|\phi\rangle$ being a pure state of the closed quantum system. In our calculation we have $\ell = L/2$ and periodic boundary conditions are used, when the two parts have $b = 2$ contact points. For brevity in the following we use the notation: $S_{\ell=L/2} = \mathcal{S}$.

1. Finite-size scaling of the maximum

The J dependence of the entanglement entropy at $h = 40.0$ is shown in Fig. 3(a) for different lengths of the chain. $\mathcal{S}(J)$ has a maximum, the position of which $J_{\max}(L)$ can be used as a finite-size, pseudo-phase-transition point [22]. It approaches the true transition point, J_c as $J_{\max}(L) - J_c \sim \ln L/L^2$. The logarithmic correction term has been detected at $h = 0$ and it seems to be present for $h > 0$ as well, which is illustrated in Fig. 3(b). Using this correction term the phase-transition point can be accurately determined. We obtained the follow-

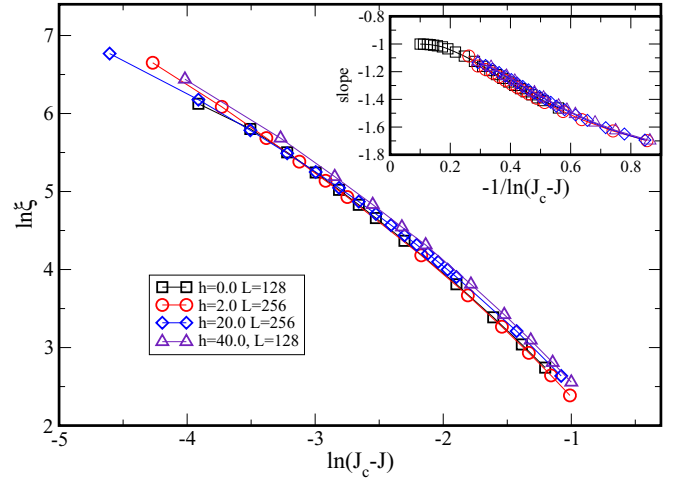


FIG. 4. The correlation length, extracted from the entropy through Eq. (11) as a function of the difference from the transition point $J < J_c$ in log-log scale for different values of h at $\Gamma = 1.5$. In the inset the local slope of the curves, approaching the critical exponent $-\nu$ is shown. For the case $h = 0$ the slope is taken from the analytical result in Ref. [23].

ing shift of the critical point close to $h = 0$ as $J_c/\Gamma - 1 \approx 0.19(h/\Gamma)^2$, in agreement with Ref. [7]. The value of the maximum $\mathcal{S}_{\max}(L)$, which is very close to $\mathcal{S}(J_c, L)$ is found to scale logarithmically:

$$\mathcal{S}_{\max}(L) \simeq b \frac{c}{6} \ln L, \quad (10)$$

which is illustrated in Fig. 3(c). At a second-order transition point for conformally invariant systems c is the central charge of the Virasoro algebra [24–26]. In Fig. 3(c) we obtained an estimate: $bc/6 \approx 0.17$. Repeating the same analysis at $h = 0.4$ a more accurate estimate is found: $bc/6 \approx 0.167$, whereas at $h = 0$ the exact value is $bc/6 = 1/6$, thus $c = 1/2$. Our numerical results about the entanglement entropy indicate that its finite-size scaling is compatible with the central charge of the Ising model not only at $h = 0$, but also for $h > 0$.

2. The correlation length

The correlation length ξ is extracted from the entanglement entropy, using the property, that in the vicinity of the critical point \mathcal{S} , behaves as

$$\mathcal{S} \simeq b \frac{c}{6} \ln \xi. \quad (11)$$

In the region with $J < J_c$ fixing $c = 1/2$ and $b = 2$ we have calculated $\ln \xi$ from Eq. (11), which are shown in Fig. 4 as a function of $\ln(J_c - J)$ for different values of h . It is seen that the curves for different h are very close to each other and therefore the same type of asymptotic scaling is expected, as for $h = 0$. We have also calculated the slope of the curves, shown in the inset of Fig. 4, which is expected to approach $-\nu = -1$, as known analytically at $h = 0$. We conclude that the correlation length critical exponent in the region with $J < J_c$ for all values of $h > 0$ is compatible with the Ising value $\nu = 1$. Expecting that this relation holds for large h , where $h/J_c \approx 2$ the asymptotic region of the numerical points is in

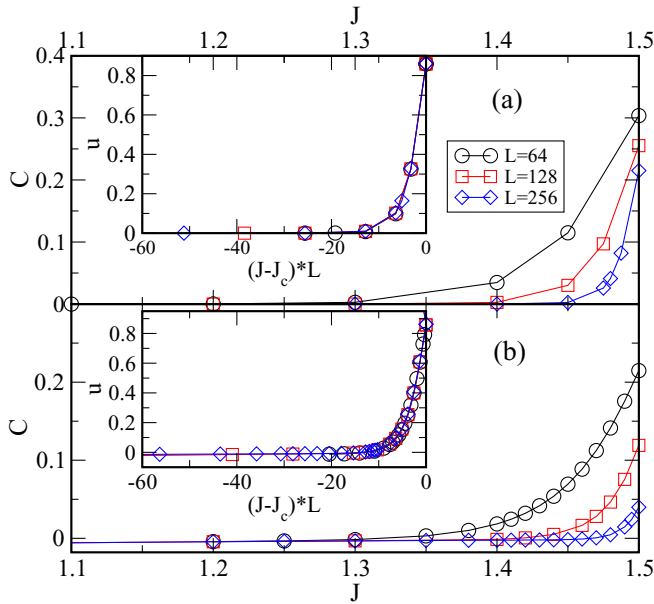


FIG. 5. Correlation function (a) at $\Gamma = 1.5$, $h = 0$ and (b) at $\Gamma = 1.5$, $h = 0.4$ as a function of the coupling for different lengths. In the insets the scaling plots $u = C(J, L)L^{1/4}$ vs $(J - J_c)L$ are shown.

accordance with the relation:

$$\xi(h) \sim \frac{\Gamma}{J_c - J} \sim \left(\frac{J_c}{J_c - J}\right) \frac{\Gamma}{J_c} \sim \Delta^{-1} \frac{\Gamma}{h_c} \sim \frac{\Gamma}{h - h_c}, \quad (12)$$

with $\Delta = (J_c - J)/J_c = (h - h_c)/h_c$ being the reduced control parameter at the transition point. Now taking $\Gamma \sim \Gamma_c$ we notice that the correlation length at the CEP tends to a finite value, since $\Gamma_c \sim (2 - h)$. In this way we have a smooth behavior of ξ around the CEP.

B. Correlation function

The order in the ground state is characterized by the correlation function in Eq. (3). In general, we consider correlations between distant points, fix $r = L/2 - 1$ and for brevity we use the notation $C(L/2 - 1) = C$, which is the function of J , Γ and h .

If there is no interaction, $J = 0$, then the correlation function is ferromagnetic, $C(J = 0) = -[(\Gamma/h)^2 + 1]^{-1} < 0$. By switching on the coupling, $J > 0$, the correlation function increases and for $J > J_c$ it becomes antiferromagnetic, $C > 0$. Numerical results of the DMRG calculations are shown in Fig. 5 for $h = 0$ in (a) and for $h = 0.4$ in (b). The curves can be scaled to a master curve by using the combination $C(J, L)L^{1/4}$ see Eq. (4) and $(J - J_c)L$ according to Eq. (2), which are shown in the insets. This scaling collapse is perfect for $h = 0$, but for $h = 0.4$ the correlation function goes below zero for sufficiently small value of J and here a more complex scenario takes place. To check this behavior we magnified the correlation function near the transition point, which is shown in Fig. 6(a) for $h = 0.4, 0.8$, and 1.2 .

It is seen in this figure that depending on the distance from the critical point J_c (which is calculated through the location of the maximum of the entanglement entropy; see in Sec. III A 1), there are two regimes below J_c . In these

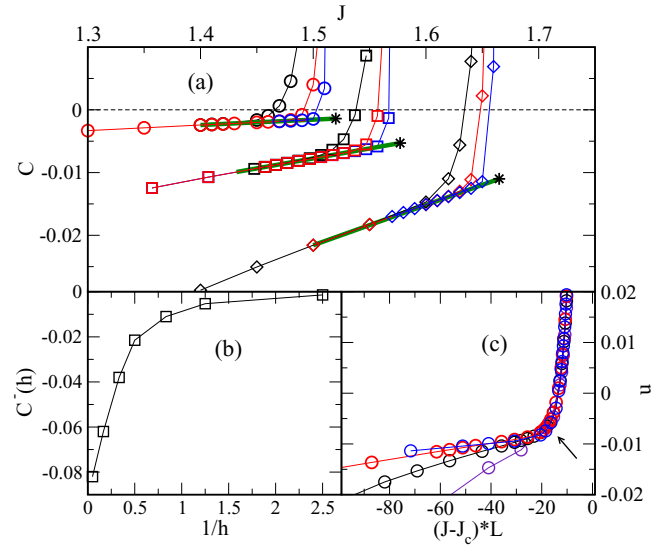


FIG. 6. (a) Correlation function at $h = 0.4$ (denoted by \circ), $h = 0.8$ (denoted by \square), and 1.2 (denoted by \diamond) for $\Gamma = 1.5$ as a function of the antiferromagnetic coupling, $J > 0$, close to the transition point, calculated by DMRG at different lengths: $L = 256$ \circ , $L = 512$ \square , $L = 1024$ \diamond . The expected form of the correlation function in the thermodynamic limit is indicated by green lines, as defined in Eq. (13); its endpoint is shown by an $*$. The limiting values $C^-(h)$ as a function of $1/h$ are plotted in (b). In (c) a scaling plot of $u = C(J, L)L^{1/4}$ vs $(J - J_c)L$ is shown for $h = 0.4$; here points for a length $L = 128$ are indicated by \circ . The point indicated by an arrow is the critical endpoint, which separates the critical and the linear regimes; see text.

regimes, the size dependence of the correlation function is different, which leads to different limiting values for $L \rightarrow \infty$. For sufficiently weak couplings, $J_c - J > \Delta J(L)$, we are in the *linear regime*, where $C(L, J)$ has an approximately linear increase with J and there is no noticeable size dependence, at least for $L \geq 128$. The other regime, which we call as *critical regime*, is located in the vicinity of the transition point for $J_c - J < \Delta J(L)$, where $C(L, J)$ grows very fast with J and there is a strong size dependence. The extent of the critical regime scales as $\Delta J(L) \sim 1/L$ [see later in Fig. 6(c)] and in the thermodynamic limit the linear regime persists up to J_c , so that we expect

$$\lim_{L \rightarrow \infty} C(L, J, h) \approx C^-(h) + a(h)(J - J_c), \quad \text{for } J \lesssim J_c, \quad (13)$$

which is indicated by dashed green lines in Fig. 6(a). The limiting value at the transition point, $C^-(h) < 0$, is ferromagnetic and its value is shown as a function of h in Fig. 6(b). For small h we notice a quadratic behavior: $|C^-(h)| \approx 0.019(h/\Gamma)^2$. The slope of the linear part $a(h)$ is found approximately proportional to $C^-(h)$: $a(h)/C^-(h) \sim -6.5$ and this proportionality factor depends only weakly on h .

In the critical regime the points in Fig. 6(a) can be put to a master curve in terms of the scaling variables: $u = C(J, L)L^{1/4}$ vs $(J - J_c)L$, which is shown in Fig. 6(c). The scaling collapse fails in the linear regime for $J_c - J > \Delta J(L)$, which sets the border of the critical region: $\Delta J(L) \sim 16/L$, where $u \sim -0.008$. Consequently in the thermodynamic limit

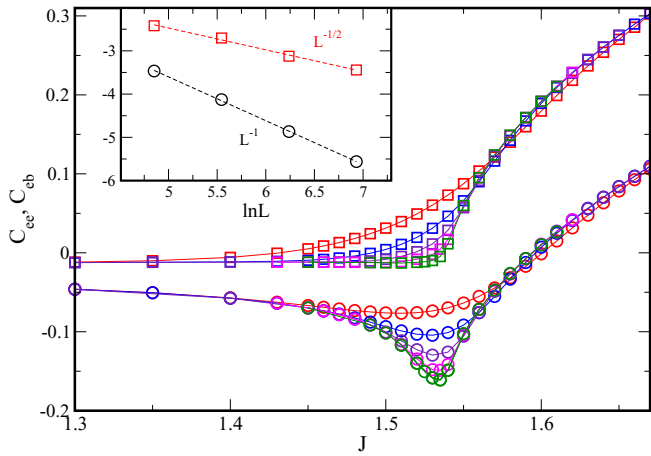


FIG. 7. End-to-end C_{ee} (denoted by \circ) and end-to-bulk C_{eb} correlation functions (denoted by \square) for $\Gamma = 1.5$ and $h = 0.4$ as a function of J for different lengths of the open chain. $L = 32$ \circ , $L = 64$ \circ , $L = 128$ \circ , $L = 256$ \circ , $L = 512$ \circ , and $L = 1024$ \circ . (Inset) Scaling of the finite-size correction to the minimum value of $[C_{ee}(J_c, L) + 0.193]$ (denoted by \square) and the radius of curvature at the minimum $\mathcal{R}(J_c)$ (denoted by \circ), as a function of L in log-log scale; see text.

$\lim_{L \rightarrow \infty} C(L, J, h) = 0$, if we stay in the critical regime: $J_c - \Delta J(L) < J \leq J_c$. Evidently this limiting value of the correlation function at the transition point is different from that extrapolated from the linear regime; see in Eq. (13).

We can conclude our numerical results in the following way. The correlation function in the thermodynamic limit is antiferromagnetic, $C(J) < 0$ for $J > J_c$ which goes to zero as $C(J) \sim [J - J_c]^{1/4}$, both at $h = 0$ and for $h > 0$. Also the correlation length is divergent with the Ising exponent, $\nu = 1$. For $h > 0$ the correlation function is discontinuous at J_c , it has a jump $C^-(h)$, as defined in Eq. (13). Consequently the phase transition is mixed order in this case.

C. End-to-end correlations

We have also studied the behavior of the end-to-end correlation function, $C_{ee} = -\langle \sigma_1^z \sigma_L^z \rangle$, which is calculated for open chains. Here we should note that the end spins are loosely connected to the chain. For example, in the classical limit, $\Gamma = 0$, C_{ee} changes sign at $h = J$, so that for $1 < h/J < 2$ we have $C_{ee} = -1$, while the bulk correlations are $C = 1$. To avoid such an independent surface transition we keep in the following $h < J$ even for $\Gamma > 0$. As an example we consider $\Gamma = 1.5$ and $h = 0.4$ and plot C_{ee} for different values of the antiferromagnetic coupling in Fig. 7. For a comparison we show in this figure also the end-to-bulk correlations, $C_{eb} = -\langle \sigma_1^z \sigma_{L/2}^z \rangle$, which is defined now with open boundary conditions. It is seen in this figure that for both types of correlations a singularity develops around the phase-transition point at $J_c = 1.52$. The end-to-end correlations show a minimum, and the value at the minimum, $C_{ee}(J_c, L)$, approaches an asymptotic value, $C_{ee}(J_c, L = \infty) \approx -0.193$ as a power: $\sim L^{-\eta_s}$ with an exponent $\eta_s \approx 0.5$. This is illustrated in the inset of Fig. 7, in which $C_{ee}(J_c, L) + 0.193$ is plotted vs L in log-log scale. In this inset we have also studied the radius of curvature at the minimum $\mathcal{R}(J)$, which is found to scale as

$\mathcal{R}(J) \sim 1/L$. We can interpret $\mathcal{R}(J)$ as the distance from the critical point in a finite system, having a correlation length $\xi \sim L$. Consequently at the transition point for the end-to-end correlations there is a diverging length, which scales with the Ising exponent $\nu = 1$, but at the same time its derivative is discontinuous in the thermodynamic limit.

For the end-to-bulk correlation function the analysis of the numerical data is more difficult. For the largest finite systems, $L = 512$ and 1024 , we notice the appearance of a minimum near the phase-transition point and we expect a similar type of behavior, as found for the end-to-end correlation function.

IV. DISCUSSION

In this paper we have re-examined the properties of the phase transition of the antiferromagnetic quantum Ising chain in the presence of a longitudinal field. Previous studies have focused on the excitation spectrum of the system and vanishing gaps are observed at the phase-transition line. Finite-size scaling of the low-energy excitations at the transition line are found to have the same behavior for $h/\Gamma > 0$ as for $h/\Gamma = 0$, i.e., at the TIM point. Therefore it was generally accepted that the phase transition for $h/\Gamma > 0$ is controlled by the TIM fixed point. Here we have studied other physical quantities of the model, entanglement entropy and spin-spin correlation function, and have clarified this issue further.

First we have introduced and applied a quantum block RG method which is known to correctly describe the properties of the TIM fixed point in the large block-size limit. Introducing a nonzero longitudinal field to the RG transformation the TIM fixed point is found unstable, signaling the possibility that the phase transition for $h/\Gamma > 0$ belongs to a different universality class. Quantitative results about the properties of the phase transition have been calculated by the DMRG method. The location of the phase-transition line is obtained as the extrapolated value of the position of the maximum of the entanglement entropy. Finite-size scaling of the entanglement entropy at the transition line is found compatible with the behavior at the TIM point, thus having a central charge $c = 1/2$. The correlation length is extracted from the scaling of the entanglement entropy and for $J < J_c$ it is found to scale as in the TIM. We have also checked (not shown here) that the transverse magnetization $\langle \sigma^x \rangle$ has the same type of singular behavior at the transition point: $\langle \sigma^x \rangle \approx c_1 + c_2(J_c - J) \ln |J_c - J|$, for $h/\Gamma > 0$, as at the TIM.

The AFM or FM order in the system is characterized by the spin-spin correlation function, what we have calculated for large periodic chains with different lengths. Starting from the AFM phase, $J > J_c$, the correlation function is found to vanish at the phase-transition point in the same form, as at the TIM, thus having the same critical exponents. Surprisingly, by passing the phase-transition line, the correlation function shows a discontinuity with a limiting finite FM value. Repeating the same calculations for the end-to-end correlations in open chains a minimum is observed at the phase-transition point having a discontinuity in the derivative. The behavior of the correlation functions around the phase-transition point is illustrated in Fig. 8 for $h = 0$ and in the inset for $h > 0$.

These findings can be interpreted that the phase transition in the antiferromagnetic quantum Ising chain in the presence

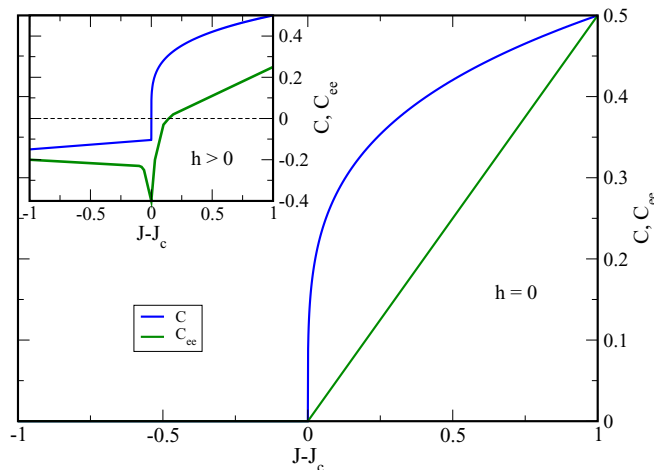


FIG. 8. Illustration of the coupling dependence of the spin-spin correlation function in the bulk (C) and between end spins (C_{ee}) at $h = 0$ (main panel) and at $h > 0$ (inset).

of a longitudinal field is of mixed order. The length scale ξ is divergent according to Eq. (2) at both sides of the transition point. Also the spin-spin correlation function shows AFM quasi-long-range order at the transition point having the TIM exponent below Eq. (4). But coming from the FM side the FM order vanishes discontinuously at the transition point.

A similar type of discontinuity occurs near the CEP point which can be evaluated by two points of view. On the one hand, being in the classical limit, $J/\Gamma \rightarrow \infty$ the correlation function has a jump from $C = -1$ to $C = 1$ at $h/J = 2$ by increasing J . On the other hand, one can observe a jump between the low-temperature limit and the small quantum fluctuation limit of the correlations at the CEP. To discuss in more detail, at the CEP point the ground state infinitely degenerate, these are denoted by $|\psi_k^{(0)}\rangle$, with $k = 1, 2, \dots, K(L)$. The entropy per site is given by

$\lim_{L \rightarrow \infty} \ln K(L)/L = \ln \tau$, with $\tau = (1 + \sqrt{5})/2$ being the golden mean ratio [9]. One can find a finite FM order by calculating the spin-spin correlation function in the low-temperature limit, when the degenerate states have equal weights, $|\Psi^{\text{therm}}\rangle = K(L)^{-1/2} \sum_k |\psi_k^{(0)}\rangle$. In the thermodynamic limit it is $C_{\text{CEP}}^{\text{therm}} = -0.2$. By switching on quantum fluctuations $1 \ll J/\Gamma < \infty$ the ground state becomes nondegenerate through an order through disorder phenomena [27] when the ground state is given as a combination of the degenerate states with well-defined weights: $|\Psi^{\text{quant}}\rangle = \sum_k c_k |\psi_k^{(0)}\rangle$. Also in this limit the correlation function maintains finite FM value $C_{\text{CEP}}^{\text{quant}} < 0$. Comparing its value with $C_{\text{CEP}}^{\text{therm}}$ we notice a jump, since $C_{\text{CEP}}^{\text{quant}} - C_{\text{CEP}}^{\text{therm}} \approx -0.16$.

Mixed-order transitions have already been observed in different systems: in classical spin chains with long-range interactions [28–35], in models of depinning transition [36–39], in percolation models with glass and jamming transition [40–49], in models at a multiple-junction or k-booklet geometry [50–53], in modular networks [54], and in experiments [55]; for a recent review see in Ref. [56]. In our model the mixed-order transition is probably the consequence of competing AFM interactions and longitudinal fields in the presence of quantum fluctuations. In an analogy we might expect that mixed-order transition takes place in the multispin version of the model [10] for $m = 3$, or in the q -state FM quantum Potts chain [57] in the presence of a q -periodic longitudinal field.

ACKNOWLEDGMENTS

This work was supported by the National Research Fund under Grants No. K128989, No. K115959, and No. KKP-126749. The authors thank J.-Ch. Anglès d’Auriac and H. Rieger for previous collaboration on this problem.

-
- [1] S. Sachdev, *Quantum Phase Transitions* (Cambridge University Press, Cambridge, 2011).
 - [2] M. Lewenstein, A. Sanpera, and V. Ahufinger, *Ultracold Atoms in Optical Lattices: Simulating Quantum Many-body Systems* (Oxford University Press, Oxford, 2012).
 - [3] J. Simon, W. S. Bakr, R. Ma, M. E. Tai, P. M. Preiss, and M. Greiner, *Nature (London)* **472**, 307 (2011).
 - [4] P. Sen, *Phys. Rev. E* **63**, 016112 (2000).
 - [5] A. A. Ovchinnikov, D. V. Dmitriev, V. Y. Krivnov, and V. O. Cheranovskii, *Phys. Rev. B* **68**, 214406 (2003).
 - [6] P. Lajkó, J.-C. A. d’Auriac, H. Rieger and F. Iglói, *Phys. Rev. B* **101**, 024203 (2020).
 - [7] Y. P. Lin, Y. J. Kao, P. Chen, and Y. C. Lin, *Phys. Rev. B* **96**, 064427 (2017).
 - [8] O. F. de Alcantara Bonfim, B. Boechat and J. Florencio, *Phys. Rev. E* **99**, 012122 (2019).
 - [9] F. Iglói, *Phys. Rev. B* **40**, 2362 (1989).
 - [10] K. A. Penson, J. M. Debierre, and L. Turban, *Phys. Rev. B* **37**, 7884 (1988).
 - [11] F. Mallezie, *Phys. Rev. B* **41**, 4475 (1990).
 - [12] F. Iglói, J. R. Heringa, M. M. F. Philippens, A. Hoogland, and H. W. J. Blöte, *J. Phys. A: Math. Gen.* **25**, 6231 (1992).
 - [13] P. Pfeuty, *Ann. Phys.* **57**, 79 (1970).
 - [14] C. Domb, *Adv. Phys.* **9**, 149 (1960).
 - [15] K. G. Wilson, *Rev. Mod. Phys.* **47**, 773 (1975).
 - [16] D. Drell, M. Weinstein, and S. Yankielowicz, *Phys. Rev. D* **14**, 487 (1976).
 - [17] P. Pfeuty, R. Jullien, K. A. Penson, in *Real Space Renormalization*, edited by T. W. Burkhardt and J. M. J. van Leeuwen (Springer, Berlin, 1982).
 - [18] K. Uzelac, R. Jullien, and P. Pfeuty, *J. Phys. A* **13**, 3735 (1980).
 - [19] F. Iglói, *Phys. Rev. B* **48**, 58 (1993).
 - [20] S. R. White, *Phys. Rev. Lett.* **69**, 2863 (1992).
 - [21] S. R. White, *Phys. Rev. B* **48**, 10345 (1993).
 - [22] F. Iglói, Y.-C. Lin, H. Rieger, and C. Monthus, *Phys. Rev. B* **76**, 064421 (2007).
 - [23] F. Iglói and Y.-C. Lin, *J. Stat. Mech.* (2008) P06004.

- [24] C. Holzhey, F. Larsen, and F. Wilczek, *Nucl. Phys. B* **424**, 443 (1994).
- [25] V. E. Korepin, *Phys. Rev. Lett.* **92**, 096402 (2004).
- [26] P. Calabrese and J. Cardy, *J. Stat. Mech.* (2004) P06002.
- [27] J. Villain, R. Bidaux, J.-P. Carton, and R. Conte, *J. Phys.* **41**, 1263 (1980).
- [28] P. W. Anderson and G. Yuval, *Phys. Rev. Lett.* **23**, 89 (1969).
- [29] D. Thouless, *Phys. Rev.* **187**, 732 (1969).
- [30] F. J. Dyson, *Commun. Math. Phys.* **21**, 269 (1971).
- [31] J. L. Cardy, *J. Phys. A* **14**, 1407 (1981).
- [32] M. Aizenman, J. T. Chayes, L. Chayes, and C. M. Newman, *J. Stat. Phys.* **50**, 1 (1988).
- [33] J. Slurink and H. Hilhorst, *Physica A*: **120**, 627 (1983).
- [34] A. Bar and D. Mukamel, *Phys. Rev. Lett.* **112**, 015701 (2014).
- [35] J-Ch. Anglès d'Auriac and F. Iglói, *Phys. Rev. E* **94**, 062126 (2016).
- [36] D. Poland and H. A. Scheraga, *J. Chem. Phys.* **45**, 1456 (1966).
- [37] M. E. Fisher, *J. Chem. Phys.* **45**, 1469 (1966).
- [38] R. Blossey and J. O. Indekeu, *Phys. Rev. E* **52**, 1223 (1995).
- [39] M. E. Fisher, *J. Stat. Phys.* **34**, 667 (1984).
- [40] D. J. Gross, I. Kanter, and H. Sompolinsky, *Phys. Rev. Lett.* **55**, 304 (1985).
- [41] C. Toninelli, G. Biroli, and D. S. Fisher, *Phys. Rev. Lett.* **96**, 035702 (2006).
- [42] C. Toninelli, G. Biroli, and D. S. Fisher, *Phys. Rev. Lett.* **98**, 129602 (2007).
- [43] J. Schwarz, A. J. Liu, and L. Chayes, *Europhys. Lett.* **73**, 560 (2006).
- [44] Y. Y. Liu, E. Csóka, H. Zhou, and M. Pósfai, *Phys. Rev. Lett.* **109**, 205703 (2012).
- [45] W. Liu, B. Schmittmann, and R. Zia, *Europhys. Lett.* **100**, 66007 (2012).
- [46] R. Zia, R. W. Liu, and B. Schmittmann, *Phys. Procedia* **34**, 124 (2012).
- [47] L. Tian and D. N. Shi, *Phys. Lett. A* **376**, 286 (2012).
- [48] G. Bizhani, M. Paczuski, and P. Grassberger, *Phys. Rev. E* **86**, 011128 (2012).
- [49] M. Sheinman, A. Sharma, J. Alvarado, G. H. Koenderink, and F. C. MacKintosh, *Phys. Rev. Lett.* **114**, 098104 (2015).
- [50] F. Iglói, L. Turban, and B. Berche, *J. Phys. A* **24**, L1031 (1991).
- [51] J. L. Cardy, *J. Phys. A* **24**, L1315 (1991).
- [52] R. Juhász and F. Iglói, *Phys. Rev. E* **95**, 022109 (2017).
- [53] P. Grassberger, *Phys. Rev. E* **95**, 010102(R) (2017).
- [54] G. Ódor and B. de Simoni, *Phys. Rev. Research* **3**, 013106 (2021).
- [55] R. Alert, P. Tierno, and J. Casademunt, *PNAS* **114**, 12906 (2017).
- [56] A. Bar and D. Mukamel, *J. Stat. Mech.* (2014) P11001.
- [57] J. Sólyom and P. Pfeuty, *Phys. Rev. B* **24**, 218 (1981).